Wavelength-selective visible-light detector based on integrated graphene transistor and surface plasmon coupler

Christian W. Smith[*a,b], Doug Maukonen[a], R. E. Peale[a], C. J. Fredricksen[a], M. Ishigami[a,b], and J. W. Cleary[c]

[a]Nanoscience Technology Center, University of Central Florida, Orlando, FL 32816;
[b]Department of Physics, University of Central Florida, Orlando FL 32816;
[c]Sensors Directorate, Air Force Research Laboratory, Wright Patterson Air Force Base, OH 45433.

ABSTRACT

We have invented a novel photodetector by mating a surface plasmon resonance coupler with a graphene field effect transistor. The device enables wavelength selectivity for spectral sensing applications. Surface plasmon polaritons (SPPs) are generated in a 50 nm thick Ag film on the surface of a prism in the Kretschmann configuration positioned 500 nm from a graphene FET. Incident photons of a given wavelength excite SPPs at a specific incidence angle. These SPP fields excite a transient current whose amplitude follows the angular resonance spectrum of the SPP absorption feature. Though demonstrated first at visible wavelengths, the approach can be extended far into the infrared. We also demonstrate that the resonant current is strongly modulated by gate bias applied to the FET, providing a clear path towards large-scale spectral imagers with locally addressable pixels.

Keywords: Surface Plasmon, Photodetector, Graphene

1. INTRODUCTION

A detector with tunable wavelength selectivity would enable compact spectral sensors with myriad defense applications. We present such a detector based on a graphene transistor coupled with a surface plasmon resonance device.

Graphene-based field effect transistors are suitable for application to ultra high speed photodetection due to short photo-excited carrier lifetime[1] and high room-temperature carrier mobility[2]. Graphene has wideband absorption[3], rapid photoresponse[4], and gives measurable photocurrents[5,6]. However, the optical absorption of graphene is weak, and the quantum efficiency of an isolated graphene layer as a detector is low. Furthermore, graphene lacks intrinsic optical selectivity[7]. There have been attempts to increase sensitivity by placing graphene in a microcavity, allowing for multiple interactions with incident radiation[8,9]. We present a method to simultaneously increase sensitivity and selectivity.

In our approach, free space electromagnetic waves are converted to bound surface plasmon polaritons (SPP) on a plane metal surface using a Kretschmann prism coupler[10, 11]. The intense evanescent fields of the SPPs penetrate a graphene FET positioned 500 nm away. The light is incident on the metal film from within the prism, which slows the light so that, at the proper angle of incidence, the in-plane component of the incident wave vector matches that of SPPs at a given optical frequency. Then, for optimized metal thickness, the incident light is converted completely into SPPs. This effect is demonstrated by zero reflectance of the incident beam at the resonance angle. Couplers can be designed for near-UV to THz wavelengths by choosing appropriate structures[12] or materials[13, 14, 15].

The dependence of resonance angle on optical frequency imparts the spectral selectivity for our graphene phototransistor. We observe a temporal current in graphene, which is sharply peaked at the SPP resonance angle. The signal-to-noise ratio is comparable to that achieved by the silicon detector that monitors the excitation beam intensity. The observed current is strongly modulated by gate bias applied to the graphene FET, suggesting a read-out scheme for future imaging arrays comparable to that of thin film transistor arrays used in active matrix displays or direct radiography imagers.

2. METHODOLOGY

Figure 1a presents a schematic of the device. It consists of a right angle N-BK7 prism coupler interfaced with a graphene FET, which sits atop 280 nm of thermal SiO_2 on silicon. A pair of 500 nm thick SiO_2 spacers separated the

graphene from the silver coated prism. These electron-beam evaporated SiO_2 standoffs at the prism edges precisely established an air gap between SPP host metal and the FET. 50 nm thick silver was deposited on the prism surface. This is approximately 1 skin depth. SPP fields penetrate the air gap and interact with the graphene. The air gap insures that the refractive index above the SPP host metal is less than that of the prism, a condition for SPP excitation.

The graphene was grown by low-pressure chemical vapor deposition (CVD) on copper[16, 17] and transferred from the copper to oxidized silicon wafers[18, 19]. The graphene was supported by sacrificial polymethyl methacrylate (PMMA) as it was etched from the copper (24 hours in 1% ammonium persulfate solution (APS)) before cleaning in baths of fresh APS and deionized water. The graphene film was patterned into 250 µm wide x 8000 µm long channels using photolithography and reactive ion etching. Au source and drain contacts are used on each end of the channel, with a third connection made to the silicon back gate. Devices were capped with a planarizing 60 nm PMMA layer before mounting to the prism coupler, yielding single-layer graphene FETs with defect density below 2 x 10^{10} cm^{-2} and ~ 1000 cm^2/V s carrier mobility, as determined via Raman spectroscopy[20, 21, 22, 23] and electrical transport measurement[24].

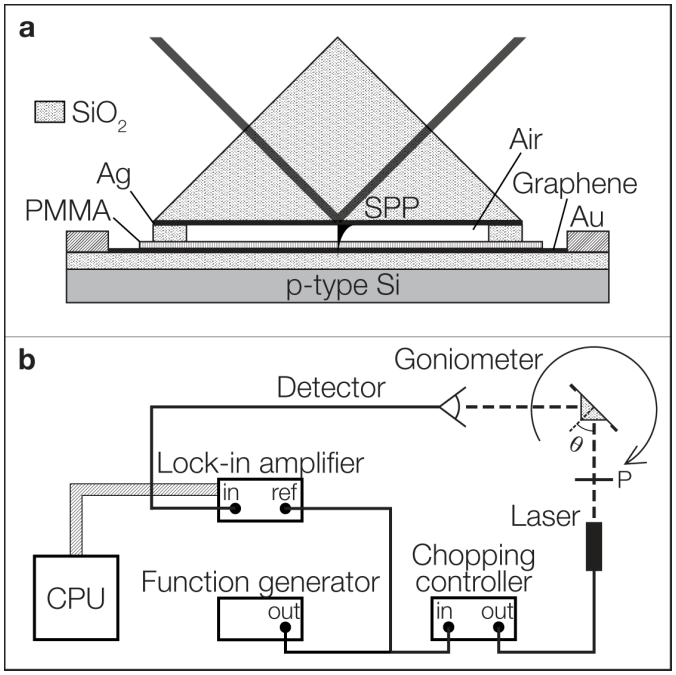

Figure 1. a) Schematic of the device under test. b) Experimental set-up.

Figure 1b presents a schematic of the experimental set up. A motorized goniometer varied the incidence angle for the TM-polarized (p-polarized) incident beam. The monochromatic light sources were a laser-diode pointer emitting at 651 nm and a diode-pumped doubled Nd-YAG laser pointer emitting at 532 nm. Wavelengths were determined by measuring the laser spectra with a Bomem DA8 Fourier spectrometer. Both sources were electrically chopped. The 2 mm diameter beam was centered on the graphene channel to minimize photocurrent generation at the electrodes[25, 26]. The specularly reflected intensity was recorded by a silicon detector and lock-in amplifier simultaneously with the response of the graphene channel.

Figure 2 presents more detail of the data acquisition electronics. The transient graphene response is preamplified before gated-boxcar integration. The integrator output is then digitized with a USB-digital to analog converter (DAC) board with custom-built labview code. An oscilloscope connected by GPIB to the computer running Labview is used to save the line shape of the transient response.

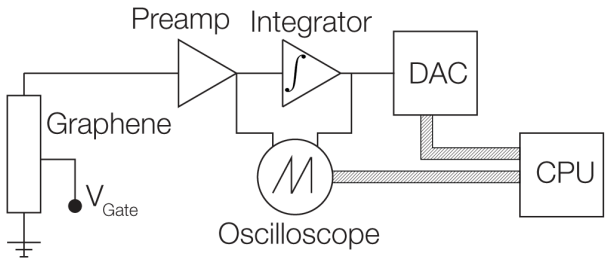

Figure 2. Details of data acquisition electronics.

3. RESULTS

Figure 3 presents measured current transients at the 42 deg angle of incidence, which is approximately the SPP resonance angle for 651 nm excitation. Solid and dashed curves correspond to TM and TE polarizations, respectively, and the latter is observed to give a much smaller effect. SPPs are excited only in the TM case, so the TE data define a non-resonant background photoresponse of ~10 nA. A peak current of ~200 nA appears for TM polarization, decaying to the background level in ~30 ms. A twice smaller negative transient occurs when the laser is chopped off. Integrating over the laser-on period we are able to capture the magnitude of the response, as the decay time does not change.

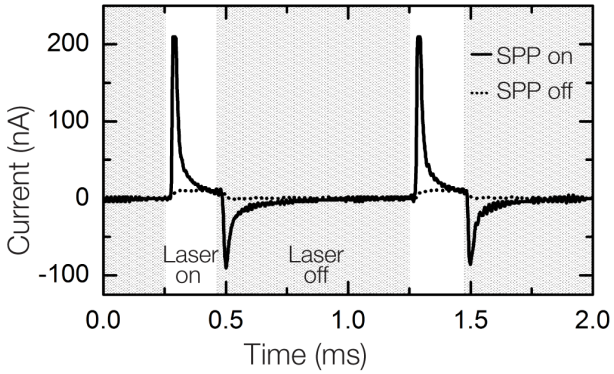

Figure 3. Current transients in the graphene channel.

Figure 4 presents plots of integrated photocurrent (solid lines) and the reflectivity (dashed lines) as a function of incidence angle for the two wavelengths. The photocurrent has been normalized by the peak response, which coincides with the SPP resonances at 42.1 and 43.5 deg for 651 and 532 nm excitation, respectively. The angular positions, depths, and widths of the SPP resonances in reflectivity are in excellent agreement with multilayer Fresnel calculations. The photocurrent closely tracks the resonance lineshapes, except that the peak photo-response occurs at slightly smaller angles. The photo-response is much larger when SPPs have been excited by TM polarization at the resonance angle than at non-resonant angles or for TE polarization. These results demonstrate wavelength selectivity based on angle tuning of the device.

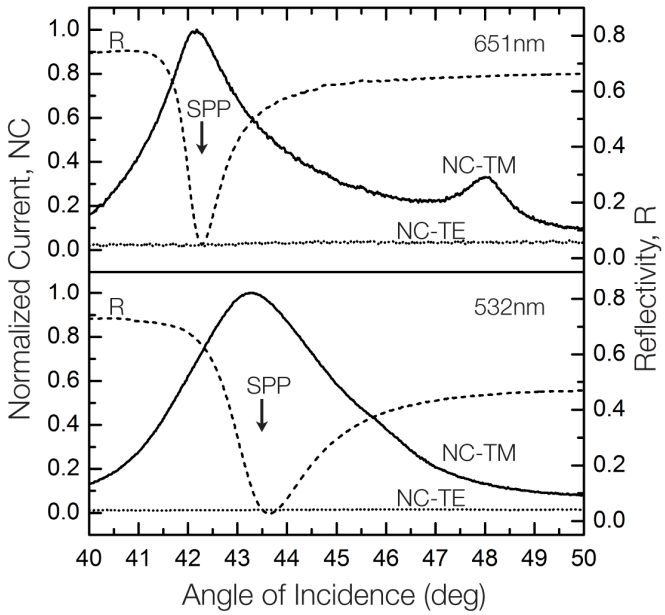

Figure 4. Photo-response of graphene FET (solid line) and specular reflectivity as a function of incidence angle. Excitation wavelengths and polarization are indicated.

We note the appearance a second weaker resonance in the photo-response at higher angles of incidence. This second peak lacks a corresponding feature in the reflectivity. At 651 nm, this feature appears by itself at 48 deg, but at 532 nm it is a shoulder at ~45.5 deg on the high angle side of the photo-resonance peak. Thus, the primary and secondary order resonances appear to move toward each other when the wavelength is decreased. The origin of the second resonance remains a puzzle.

Gate bias drastically amplifies or reduces the photoresponse magnitude and linewidth, without changing the angular position of the peak. Figure 5 presents a plot of peak photocurrent vs. gate bias. The amplitude of the response increases with increasing negative gate bias, which increases the p-type carrier concentration in the graphene. The photocurrent drops below the noise level for positive gate biases beyond ~0.4 V. The graphene is heavily p-doped[27], so that the transition to zero photo-response is uncorrelated with the charge neutrality point. However, the ability to electrically turn off the photoresponse with modest bias suggests a means of individually addressing pixels in an array detector as is done with thin-film transistor arrays in active matrix displays and direct radiography imagers.

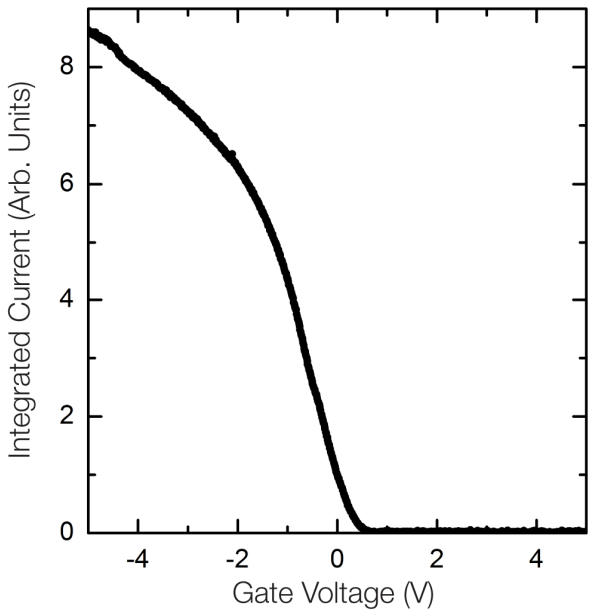

Figure 5. Gate dependence of the integrated response in the graphene channel at the SPP resonance angle.

4. CONCLUSIONS

We have presented a novel means of enhancing graphene photo-response while simultaneously achieving wavelength selectivity. The device is a marriage of two known technologies, the graphene FET and the SPP prism coupler. The specifics of our observed response have not been reported in graphene previously. Our demonstration of wavelength tunable room-temperature with excellent signal-to-noise ratio in the visible spectrum can be adapted to infrared and THz wavelengths by suitable choice of SPP coupler[11] and materials with infrared plasma frequencies[12,13,14]. Arrays with electrically addressable pixels and angle tuned wavelength selection are a clear possibility for applications in chem-bio spectral sensing.

Detailed accomplishments are as follows. We achieved electronic detection of surface plasmon polaritons. We achieved precise positioning of sensor devices within 500 nm of the SPP-generating surface using a scalable technique. We achieved spectral resolution. We positioned graphene-based devices measuring 8 mm by 250 microns only 500 nm away from the SPP-producing surface while retaining full functionality of the device. We used graphene to gate the detection, leading to a new locally addressable SPP detection technology.

ACKNOWLEDGMENTS

This work was supported by Air Force Research Laboratory under contract number FA865013C1528 and Air Force Office of Scientific Research (Program Officer Dr. Gernot Pomrenke) under contract number 12RY10COR.

REFERENCES

[1] Dawlaty, J. M., Shivaraman, S., Chandrashekhar, M., Rana, F., and Spencer, M. G., “Measurement of ultrafast carrier dynamics in epitaxial graphene,” Applied Physics Letters, 92, 042116 (2008).
[2] Chen, J.-H., Jang, C., Xiao, S., Ishigami, M., and Fuhrer, M. S., “Intrinsic and extrinsic performance limits of graphene devices on SiO2,” Nature Nanotechnology, 3(4), 206-209 (2008).

[3] Bonaccorso, F., Sun, Z., Hasan, T., and Ferrari, A., "Graphene photonics and optoelectronics," Nature Photonics, 4(9), 611-622 (2010).
[4] Xia, F., Mueller, T., Lin, Y.-m., Valdes-Garcia, A., and Avouris, P., "Ultrafast graphene photodetector," Nature Nanotechnology, 4(12), 839-843 (2009).
[5] Mueller, T., Xia, F., and Avouris, P., "Graphene photodetectors for high-speed optical communications," Nature Photonics, 4(5), 297-301 (2010).
[6] Song, J. C., Rudner, M. S., Marcus, C. M., and Levitov, L. S., "Hot carrier transport and photocurrent response in graphene," Nano Letters, 11(11), 4688-4692 (2011).
[7] Horng, J., Chen, C.-F., Geng, B., Girit, C., Zhang, Y., Hao, Z., Bechtel, H. A., Martin, M., Zettl, A., and Crommie, M. F., "Drude conductivity of Dirac fermions in graphene," Physical Review B, 83(16), 165113 (2011).
[8] Furchi, M., Urich, A., Pospischil, A., Lilley, G., Unterrainer, K., Detz, H., Klang, P., Andrews, A. M., Schrenk, W., and Strasser, G., "Microcavity-integrated graphene photodetector," Nano Letters, 12(6), 2773-2777 (2012).
[9] Engel, M., Steiner, M., Lombardo, A., Ferrari, A. C., Löhneysen, H. v., Avouris, P., and Krupke, R., "Light–matter interaction in a microcavity-controlled graphene transistor," Nature Communications, 3, 906 (2012).
[10] Kretschmann, E., "Die bestimmung optischer konstanten von metallen durch anregung von oberflächenplasmaschwingungen," Zeitschrift für Physik, 241(4), 313-324 (1971).
[11] Peale, R. E., Lopatiuk, O., Cleary, J., Santos, S., Henderson, J., Clark, D., Chernyak, L., Winningham, T. A., Barco, E. D., and Heinrich, H., "Propagation of high-frequency surface plasmons on gold," Journal of Optical Society of America B, 25(10), 1708-1713 (2008).
[12] Cleary, J. W., Medhi, G., Peale, R. E., and Buchwald, W. R., "Long-wave infrared surface plasmon grating coupler," Applied Optics, 49(16), 3102-3110 (2010).
[13] Cleary, J., Peale, R., Shelton, D., Boreman, G., Smith, C., Ishigami, M., Soref, R., Drehman, A., and Buchwald, W., "IR permittivities for silicides and doped silicon," Journal of Optical Society of America B, 27(4), 730-734 (2010).
[14] Shahzad, M., Medhi, G., Peale, R. E., Buchwald, W. R., Cleary, J. W., Soref, R., Boreman, G. D., and Edwards, O., "Infrared surface plasmons on heavily doped silicon," Journal of Applied Physics, 110(12), 123105-123105-6 (2011).
[15] Cleary, J. W., Medhi, G., Shahzad, M., Rezadad, I., Maukonen, D., Peale, R. E., Boreman, G. D., Wentzell, S., and Buchwald, W. R., "Infrared surface polaritons on antimony," Optics Express, 20(3), 2693-2705 (2012).
[16] Li, X., Cai, W., An, J., Kim, S., Nah, J., Yang, D., Piner, R., Velamakanni, A., Jung, I., and Tutuc, E., "Large-area synthesis of high-quality and uniform graphene films on copper foils," Science, 324(5932), 1312-1314 (2009).
[17] Li, X., Magnuson, C. W., Venugopal, A., An, J., Suk, J. W., Han, B., Borysiak, M., Cai, W., Velamakanni, A., and Zhu, Y., "Graphene films with large domain size by a two-step chemical vapor deposition process," Nano Letters, 10(11), 4328-4334 (2010).
[18] Reina, A., Jia, X., Ho, J., Nezich, D., Son, H., Bulovic, V., Dresselhaus, M. S., and Kong, J., "Large area, few-layer graphene films on arbitrary substrates by chemical vapor deposition," Nano Letters, 9(1), 30-35 (2008).
[19] Li, X., Zhu, Y., Cai, W., Borysiak, M., Han, B., Chen, D., Piner, R. D., Colombo, L., and Ruoff, R. S., "Transfer of large-area graphene films for high-performance transparent conductive electrodes," Nano Letters, 9(12), 4359-4363 (2009).
[20] Cancado, L., Takai, K., Enoki, T., Endo, M., Kim, Y., Mizusaki, H., Jorio, A., Coelho, L., Magalhaes-Paniago, R., and Pimenta, M., "General equation for the determination of the crystallite size La of nanographite by Raman spectroscopy," Applied Physics Letters, 88(16), 163106-163106-3 (2006).
[21] Pisana, S., Lazzeri, M., Casiraghi, C., Novoselov, K. S., Geim, A. K., Ferrari, A. C., and Mauri, F., "Breakdown of the adiabatic Born–Oppenheimer approximation in graphene," Nature Materials, 6(3), 198-201 (2007).
[22] Das, A., Pisana, S., Chakraborty, B., Piscanec, S., Saha, S., Waghmare, U., Novoselov, K., Krishnamurthy, H., Geim, A., and Ferrari, A., "Monitoring dopants by Raman scattering in an electrochemically top-gated graphene transistor," Nature Nanotechnology, 3(4), 210-215 (2008).
[23] Ferrari, A., Meyer, J., Scardaci, V., Casiraghi, C., Lazzeri, M., Mauri, F., Piscanec, S., Jiang, D., Novoselov, K., and Roth, S., "Raman spectrum of graphene and graphene layers," Physical Review Letters, 97(18), 187401 (2006).
[24] Novoselov, K. S., Geim, A. K., Morozov, S., Jiang, D., Zhang, Y., Dubonos, S., Grigorieva, I., and Firsov, A., "Electric field effect in atomically thin carbon films," Science, 306(5696), 666-669 (2004).
[25] Echtermeyer, T., Britnell, L., Jasnos, P., Lombardo, A., Gorbachev, R., Grigorenko, A., Geim, A., Ferrari, A., and Novoselov, K., "Strong plasmonic enhancement of photovoltage in graphene," Nature Communications, 2, 458 (2011).

[26] Liu, Y., Cheng, R., Liao, L., Zhou, H., Bai, J., Liu, G., Liu, L., Huang, Y., and Duan, X., "Plasmon resonance enhanced multicolour photodetection by graphene," Nature Communications, 2, 579 (2011).

[27] Pirkle, A., Chan, J., Venugopal, A., Hinojos, D., Magnuson, C., McDonnell, S., Colombo, L., Vogel, E., Ruoff, R., and Wallace, R., "The effect of chemical residues on the physical and electrical properties of chemical vapor deposited graphene transferred to SiO_2," Applied Physics Letters, 99(12), 122108-122108-3 (2011).